Betaine-homocysteine *S*-methyltransferase deficiency causes increased susceptibility to noise-induced hearing loss associated with plasma hyperhomocysteinemia

Teresa Partearroyo,[*,†,1] Silvia Murillo-Cuesta,[†,‡,§,1,2] Néstor Vallecillo,[†,1] Jose M. Bermúdez-Muñoz,[†,‡] Lourdes Rodríguez-de la Rosa,[†,‡,§] Giacomo Mandruzzato,[¶] Adelaida M. Celaya,[†,‡] Steven H. Zeisel,[‖] María A. Pajares,[†,§,#] Gregorio Varela-Moreiras,[*,†] and Isabel Varela-Nieto[†,‡,§]

[*]Departamento de Ciencias Farmacéuticas y de la Salud, Facultad de Farmacia, Universidad Centro de Estudios Universitarios CEU San Pablo, Madrid, Spain; [†]Instituto de Investigaciones Biomédicas Alberto Sols, Consejo Superior de Investigaciones Científicas–Universidad Autónoma de Madrid (CSIC-UAM), Madrid, Spain; [‡]Centro de Investigación Biomédica en Red de Enfermedades Raras, (CIBERER), Instituto de Salud Carlos III, Madrid, Spain; [§]Instituto de Investigación Sanitaria La Paz (IdiPAZ), Madrid, Spain; [¶]Research and development, MED-EL, Innsbruck, Austria; [‖]Nutrition Research Institute, University of North Carolina at Chapel Hill, Kannapolis, North Carolina, USA; and [#]Centro de Investigaciones Biológicas, (CSIC) Madrid, Spain

ABSTRACT: Betaine-homocysteine *S*-methyltransferases (BHMTs) are methionine cycle enzymes that remethylate homocysteine; hence, their malfunction leads to hyperhomocysteinemia. Epidemiologic and experimental studies have revealed a correlation between hyperhomocysteinemia and hearing loss. Here, we have studied the expression of methionine cycle genes in the mouse cochlea and the impact of knocking out the *Bhmt* gene in the auditory receptor. We evaluated age-related changes in mouse hearing by recording auditory brainstem responses before and following exposure to noise. Also, we measured cochlear cytoarchitecture, gene expression by RNA-arrays and quantitative RT-PCR, and metabolite levels in liver and plasma by HPLC. Our results indicate that there is an age-dependent strain-specific expression of methionine cycle genes in the mouse cochlea and a further regulation during the response to noise damage. Loss of *Bhmt* did not cause an evident impact in the hearing acuity of young mice, but it produced higher threshold shifts and poorer recovery following noise challenge. Hearing loss was associated with increased cochlear injury, outer hair cell loss, altered expression of cochlear methionine cycle genes, and hyperhomocysteinemia. Our results suggest that BHMT plays a central role in the homeostasis of cochlear methionine metabolism and that *Bhmt2* up-regulation could carry out a compensatory role in cochlear protection against noise injury in the absence of BHMT.—Partearroyo, T., Murillo-Cuesta, S., Vallecillo, N., Bermúdez-Muñoz, J. M., Rodríguez-de la Rosa, L., Mandruzzato, G., Celaya, A. M., Zeisel, S. H., Pajares, M. A., Varela-Moreiras, G., Varela-Nieto, I. Betaine-homocysteine *S*-methyltransferase deficiency causes increased susceptibility to noise-induced hearing loss associated with plasma hyperhomocysteinemia. FASEB J. 33, 5942–5956 (2019). www.fasebj.org

KEY WORDS: ARHL · cochlear injury · methionine cycle · NIHL

ABBREVIATIONS: ABR, auditory brainstem response; AdoHcy, *S*-adenosylhomocysteine; AdoMet, *S*-adenosylmethionine; *Ahcy*, AdoHcy hydrolase; BHMT, betaine-homocysteine *S*-methyltransferase; CBS, cystathionine β-synthase; *Gclc*, glutamate-cysteine ligase, catalytic subunit; *Gclm*, glutamate-cysteine ligase, modifier subunit; *Hprt*, hypoxanthine-guanine phosphoribosyltransferase; *Kcnj10*, potassium voltage-gated channel subfamily J member 10; *Mat2a*, methionine adenosyltransferase II, α subunit; *Mat2b*, methionine adenosyltransferase II, β subunit; *Mtr*, methionine synthase [5-methyltetrahydrofolate-homocysteine methyltransferase]; *Mpz*, Myelin protein zero; *NeuN*, neuronal nuclei; qRT-PCR, quantitative RT-PCR; *RbFox3*, RNA binding fox-1 homolog 3; *Sox2*, sex determining region Y-box 2

[1] These authors contributed equally to this work.

[2] Correspondence: Instituto de Investigaciones Biomédicas Alberto Sols (CSIC-UAM), Arturo Duperier 4, 28029 Madrid, Spain. E-mail: smurillo@iib.uam.es

doi: 10.1096/fj.201801533R

This article includes supplemental data. Please visit *http://www.fasebj.org* to obtain this information.

Nutritional imbalance is an emerging causative factor for hearing loss (1), and a growing number of reports associate deficits in essential nutrients with human auditory dysfunction (2, 3). In particular, epidemiologic studies have linked alterations in methionine metabolism caused by folic acid and vitamin B_{12} deficiencies with age-related (4, 5), noise-induced (6), or sudden hearing loss (7). Furthermore, studies in rodents have provided some of the genetic and molecular clues to understand how micronutrient deficits impact hearing (8–11). Thus, several studies have shown that decreased folate or vitamin B_{12} levels are usually associated with increased homocysteine concentration (6, 7), a well-known independent risk factor for cardiovascular disease. Interestingly, the relationship between coronary disease, inner ear atherosclerosis, and hearing loss was described several years ago (12–14).

0892-6638/19/0033-5942 © FASEB

Moreover, clinical trials have demonstrated that supplementation with folic acid decreases plasma homocysteine levels and concomitantly slows the decline in hearing in the elderly (15, 16). Age-related and noise-induced hearing loss share certain molecular mechanisms that favor injury expansion; for example, excessive exposure to noise triggers oxidative stress, inflammation, and alterations in cochlear metabolism (17, 18). Specifically, oxidative stress, which encompasses overproduction of reactive species and depletion of antioxidants like glutathione, is the main mechanism in auditory damage by ototoxic agents. This could be a fundamental factor in their ototoxicity because glutathione protects the cochlea from noise-induced injury (19, 20).

Regarding hyperhomocysteinemia, a medical condition characterized by abnormally high levels of plasma homocysteine, several data strongly imply its association with the development of neurologic disorders, chronic kidney disease, osteoporosis, gastrointestinal disorders, cancer, and congenital defects (21–25). Lately, epidemiologic studies provided evidence of the association between atherosclerosis in the inner ear and hearing loss (12, 13), as well as between hyperhomocysteinemia and impaired cochlear blood supply (26), thus connecting risk factors for vascular disease with age-related hearing loss.

Modifications in homocysteine levels can result from defects in its catabolism through the trans-sulfuration pathway, remethylation, and export to the plasma. Increased trans-sulfuration and excretion are normally favored when methionine levels are high, whereas a need for this essential sulfur amino acid leads to increased remethylation. The balance between these steps is essential for the maintenance of methionine concentrations and, in turn, of *S*-adenosylmethionine (AdoMet) levels. In fact, under methionine excess, the consequent increase in AdoMet concentrations activates cysthationine β-synthase (CBS), the first enzyme of the trans-sulfuration pathway responsible for homocysteine transformation into cystathionine. This metabolite is then utilized by cystathionine γ-lyase to produce cysteine that contributes to glutathione synthesis. AdoMet further contributes to homocysteine methylation by its inhibitory role on the expression of one of the enzymes catalyzing this reaction, betaine-homocysteine *S*-methyltransferase (BHMT) (27, 28). This enzyme uses betaine as the methyl donor, and hence not only collaborates in homocysteine recycling but also in the recovery of one of the methylation equivalents required for phosphatidylcholine synthesis through the transmethylation pathway (1, 29).

Here, we studied the cochlear expression of genes of the methionine cycle at different ages and in response to noise stress. Our hypothesis is that a cochlear methionine well-balanced metabolism may be essential in the resilience of this sensory organ during the response to injury. The relevance of the cochlear remethylation pathway has been further studied by analyzing the impact of deleting *Bhmt* on the onset of hearing loss and the response to noise. Our results show that *Bhmt*$^{-/-}$ mice, which have much higher homocysteine concentrations in liver and plasma, exhibit alterations in cochlear homocysteine metabolism and increased susceptibility to noise-induced injury.

MATERIALS AND METHODS

Mouse handling and experimental design

C57BL/6J (Charles River Laboratories, Wilmington, MA, USA) and mixed HsdOla:MF1 (Envigo, Huntingdon, United Kingdom)–129S6/SvEvTac (Taconic Biosciences, Rensselaer, NY, USA) (MF1:129Sv) mouse strains were used for the study of cochlear expression of methionine cycle genes along life. *Bhmt*$^{-/-}$ mice (*Bhmt*$^{tm1.2Zei}$/*Bhmt*$^{tm1.2Zei}$, Resource Research Identifier MMRRC_037641-UNC) were generated in 129P2/OlaHsd–C57BL/6 background (30) and then backcrossed for more than 10 generations onto a C57BL/6J background (99.74% congenic). A total of 104 *Bhmt*$^{-/-}$ and 91 *Bhmt*$^{+/+}$ mice generated by crossing *Bhmt*$^{-/+}$ mice were used in this study. Mouse genotypes were identified using the RedExtract-N-Amp Tissue PCR Kit (MilliporeSigma, Burlington, MA, USA) according to the manufacturer's instructions. PCR was performed as follows: 1 cycle of 94°C for 2 min; 35 cycles of 94°C for 30 s, 66°C for 2 min, 72°C for 2 min; and a final elongation step at 72°C for 7 min. The wild-type *Bhmt* band was amplified using 5′-GACTTTTAAAGAGTGGTGGTACATACCTTG-3′ and 5′-TCTCTCTGCAGCCACATCTGAACTTGTCTG-3′ primers, and the knockout with 5′-TTAACTCAACATCACAACAACAGATTTCAG-3′ and 5′-TTGTCGACGGATCCATAACTTCGTATAAT-3′ primers, producing 1600- and 545-bp amplicons, respectively, as reported by Teng *et al.* (30).

All experiments were approved by the Consejo Superior de Investigaciones Científicas (CSIC) Bioethics Committee and carried out in full accordance with European Community guidelines (2010/63/EU) and Spanish regulations (RD 53/2013) for the use of laboratory animals.

Hearing assessment and noise exposure

Hearing was evaluated in *Bhmt*$^{-/-}$ and *Bhmt*$^{+/+}$ mice by recording the evoked auditory brainstem response (ABR) to sound with a System III Evoked Potential Workstation (Tucker-Davis Technologies, Alachua, FL, USA), as reported in refs. 31 and 32. Briefly, mice were anesthetized with ketamine (100 mg/kg) and xylazine (10 mg/kg) and placed on a heating pad inside a soundproof acoustic chamber. Click and 8-, 16-, 20-, 28-, and 40-kHz pure tone stimuli were presented at a decreasing intensity range from 90 to 20 dB SPL. The electroencephalographic activity was recorded, amplified, and averaged to determine hearing thresholds, latencies, and amplitudes of the evoked waves.

To evaluate susceptibility to cochlear injury, 2.5-mo-old *Bhmt*$^{-/-}$ ($n = 23$) and *Bhmt*$^{+/+}$ ($n = 24$) mice were exposed to violet swept sine noise at 105 dB SPL for 30 min, as described by Murillo-Cuesta *et al.* (18). Noise level was selected in order to produce a moderate and partially reversible hearing loss. The effect of noise exposure on hearing was evaluated by recording the evoked ABR before (baseline) and 2, 14, and 28 d after exposure.

Metabolite determinations

Blood samples were obtained by cardiac puncture after barbiturate overdose and placed in heparin-coated tubes to separate the plasma fraction by centrifugation. The liver was also quickly removed after euthanization. Plasma and liver samples were kept at −80°C until analyzed.

Plasma homocysteine was determined after derivatization using the Homocysteine in Serum/Plasma – HPLC reagent kit

(Chromsystems Instruments & Chemicals, Gräfelfing, Germany). Derivatized samples (50 μl) were injected into the HPLC column, and fluorescence was measured at 515 nm after excitation at 385 nm. Hepatic AdoMet and *S*-adenosylhomocysteine (AdoHcy) levels were determined by HPLC essentially as described by Fell *et al.* (33). Frozen liver samples (~100 mg) were homogenized in 3 volumes of 0.4 M $HClO_4$ and then centrifuged at 1000 *g* at 4°C for 10 min. The supernatant was removed, filtered, and analyzed for metabolite content. Protein concentration was determined by Pierce BCA Protein Assay Kit (Thermo Fisher Scientific, Waltham, MA USA) using external standards.

Cochlear morphology

Mice were euthanized by barbiturate overdose and then perfused with PBS and 4% (w/v) paraformaldehyde (Merck, Kenilworth, NJ, USA). Cochleae were dissected, fixed overnight, decalcified with EDTA (MilliporeSigma) for 7 d, and then dehydrated and embedded in paraffin wax (PanReac AppliChem, Barcelona, Spain), as previously described by Martínez-Vega *et al.* (10). Paraffin sections (7 μm) were stained with hematoxylin and eosin (MilliporeSigma), and photomicrographs were obtained using an DP70 digital camera (Olympus, Tokyo, Japan) mounted on a Zeiss microscope (Carl Zeiss, Oberkochen, Germany).

For counting hair cell numbers, organs of Corti of postfixed and decalcified cochleae were dissected into half-turns. The pieces were permeabilized with 1% (v/v) Triton X-100 (MilliporeSigma), blocked with 5% (v/v) normal donkey serum (MilliporeSigma), and incubated overnight at 4°C with rabbit anti–Myosin VIIA [1:150 (v/v), PT-25-6790; Proteus, Ramona, CA, USA] and Alexa Fluor secondary antibody at 1:200 (v/v) for 3 h at room temperature. The half-turns were then incubated with DAPI [1:1000 (v/v); Thermo Fisher Scientific] and mounted with Prolong (Thermo Fisher Scientific), and low-magnification fluorescent images were taken with a 90i microscope (Nikon, Tokyo, Japan). The cochleagram was plotted using these images and a free custom Fiji (*https://fiji.sc/#*) plugin as reported by Liberman *et al.* (34). Fluorescent stack images were taken with confocal microscope (LSM710; Carl Zeiss) with a glycerol-immersion objective (×40) and image spacing in the z plane of 3 μm. The number of inner and outer hair cells was quantified at specified cochlear regions (8, 16, 20, 28, 32, 40, and 48 kHz) using Fiji software in 200 μm of segments from 3 mice of each genotype.

Protein extraction and Western blotting

Cochleae were dissected and immediately frozen in liquid nitrogen for protein or RNA extraction as reported by de Iriarte Rodríguez *et al.* (17). Whole cochlear protein was prepared using the ReadyPrep Protein Extraction (Total Protein) (Bio-Rad, Hercules, CA, USA), and the concentration was determined using the RC DC Protein Assay kit (Bio-Rad) and bovine serum albumin as standard. Samples (~100 μg) were loaded on Mini-Protean TGX 10% precast polyacrylamide gels (Bio-Rad) and electrotransferred to PVDF membranes (Bio-Rad) with the Trans-Blot Turbo transfer starter system (Bio-Rad) for incubation with rabbit polyclonal anti-BHMT (1:5000 v/v) (35) and mouse polyclonal anti-CBS (1:2500 v/v, H00000875-A01; Abnova, Taipei, Taiwan) antibodies. Signals were obtained using Clarity Western ECL Substrate (Bio-Rad), captured using ImageQuant LAS4000 mini system (GE Healthcare, Waukesha, WI, USA), and quantified with the ImageQuant TL software (GE Healthcare) as reported by de Iriarte Rodríguez *et al.* (17). A β-actin signal was used for normalization.

RNA extraction, RNA array, and quantitative RT-PCR

Gene expression of methionine metabolism genes was determined by RNA-array hybridization and by quantitative RT-PCR (qRT-PCR), as reported by Sanchez-Calderon *et al.* (36). Total cochlear RNA was extracted by using the RNeasy kit (Qiagen, Hilden, Germany) and quantified on a Bioanalyzer 2100 (Agilent Technologies, Santa Clara, CA, USA).

For RNA-array hybridization, RNA was isolated from 3 independent pools of 4 cochleae obtained from 2 C57BL/6J E18.5 mice, and the expression profile was analyzed using GeneChip Mouse Genome 430A2.0 Array (Thermo Fisher Scientific) as described by Sanchez-Calderon *et al.* (36). The results were deposited in the National Center for Biotechnology Information (Bethesda, MD, USA) Gene Expression Omnibus (*http://www.ncbi.nlm.nih.gov/geo/*) and are accessible through Gene Expression Omnibus Series accession number GSE11821. Gene expression levels were estimated by 2 methods integrated in the puma Bioconductor package (37). MultimgMOS associated credibility intervals with expression levels, and subsequently, the Probability of Positive Log Ratio (PPLR) method estimated the expression levels within each condition (*https://bioconductor.org/packages/release/bioc/html/puma.html*) (36).

qRT-PCR studies were performed in RNA samples obtained from pools of 3 cochleae from 3 C57BL/6J and MF1:129Sv mice at different ages from embryonic to adult stages and also from $Bhmt^{-/-}$ and $Bhmt^{+/+}$ mice nonexposed to noise or 28 d after noise exposure. TaqMan Gene Expression Assays (Thermo Fisher Scientific) were used for amplification of homocysteine metabolism genes {AdoHcy hydrolase (*Ahcy*), *Bhmt*, *Bhmt2*, *Cbs*, glutamate-cysteine ligase, catalytic subunit (*Gclc*), glutamate-cysteine ligase, modifier subunit (*Gclm*), methionine adenosyltransferase II, α subunit (*Mat2a*), methionine adenosyltransferase II, β subunit (*Mat2b*), and methionine synthase [5-methyltetrahydrofolate-homocysteine methyltransferase] (*Mtr*)}. Similarly, gene expression levels of selected cochlear cell–type biomarkers were measured by qRT-PCR before and 28 d after noise exposure. RNA binding fox-1 homolog 3 (*RbFox3*) [neuronal nuclei (*NeuN*)] nuclear factor is expressed in postmitotic neurons and is involved in the maintenance of neuronal functions (38, 39) and was used as a marker of spiral ganglion neurons. Myelin protein zero (*Mpz*) codifies for the major component of the peripheral nervous system myelin sheath and is expressed in the spiral ganglion and cochlear nerve Schwann cells (40, 41). The transcription factor sex determining region Y-box 2 (*Sox2*) is expressed by Schwan and supporting cells in the adult cochlea (42–44). Potassium voltage-gated channel subfamily J member 10 (*Kcnj10*) encodes an inwardly rectifying potassium channel and was used as a marker of the stria vascularis intermediate cells (45). Finally, prestin [solute carrier family 26 member 5 (Slc26a5)] codifies for the homonymous motor protein specifically expressed in outer hair cells for outer hair cells (46, 47). Hypoxanthine-guanine phosphoribosyltransferase (*Hprt*) or ribosomal protein large P0 were used as endogenous control genes. The relative quantification values were determined by the $2^{-\Delta\Delta Ct}$ method, as reported by Sanchez-Calderon *et al.* (36).

Statistical analysis

Statistical analysis was performed with IBM SPSS Statistics for Windows (IBM, Armonk, NY, USA). Sample size was estimated to obtain a 90% statistical power with a significance level of 0.05, using data from previous experiments and calculating the Cohen's *d* value. Data distribution was analyzed by the Shapiro-Wilk test and visualization of the histograms and Q-Q and box plots. Either nonparametric Mann-Whitney *U* or Kruskal-Wallis tests, or parametric Student's *t* test were applied when data distribution was not normal or normal, respectively. Statistically significant differences were calculated between E.18.5 and the other temporal points in the longitudinal gene expression studies, or between $Bhmt^{-/-}$

and $Bhmt^{+/+}$ mouse groups in the rest of the experiments. Association between ABR threshold and other variables was calculated by the Pearson correlation coefficient. Results were expressed as the mean ± SEM, and differences were considered significant when $P \leq 0.05$.

RESULTS

The cochlear expression of methionine metabolism genes is age regulated

The expression of genes involved in methionine and homocysteine metabolism, including those belonging to the methionine cycle, the folate cycle, the trans-sulfuration pathway, and glutathione synthesis route, was studied using a combination of RNA array and qRT-PCR techniques in mouse cochleae from embryonic to adult stages in 2 mouse strains (**Figs. 1** and **2** and **Table 1**).

Initially, the cochlear expression of the genes of interest along age was analyzed by qRT-PCR on the mouse strain MF1:129Sv. Transcripts from *Ahcy*, *Mat2a*, and *Mat2b* genes, involved in homocysteine synthesis, showed higher expression levels in the embryonic than in the postnatal cochlea, these levels decreasing progressively with age (Fig. 1). Expression of *Mtr*, responsible for homocysteine remethylation using folate, displayed a similar pattern,

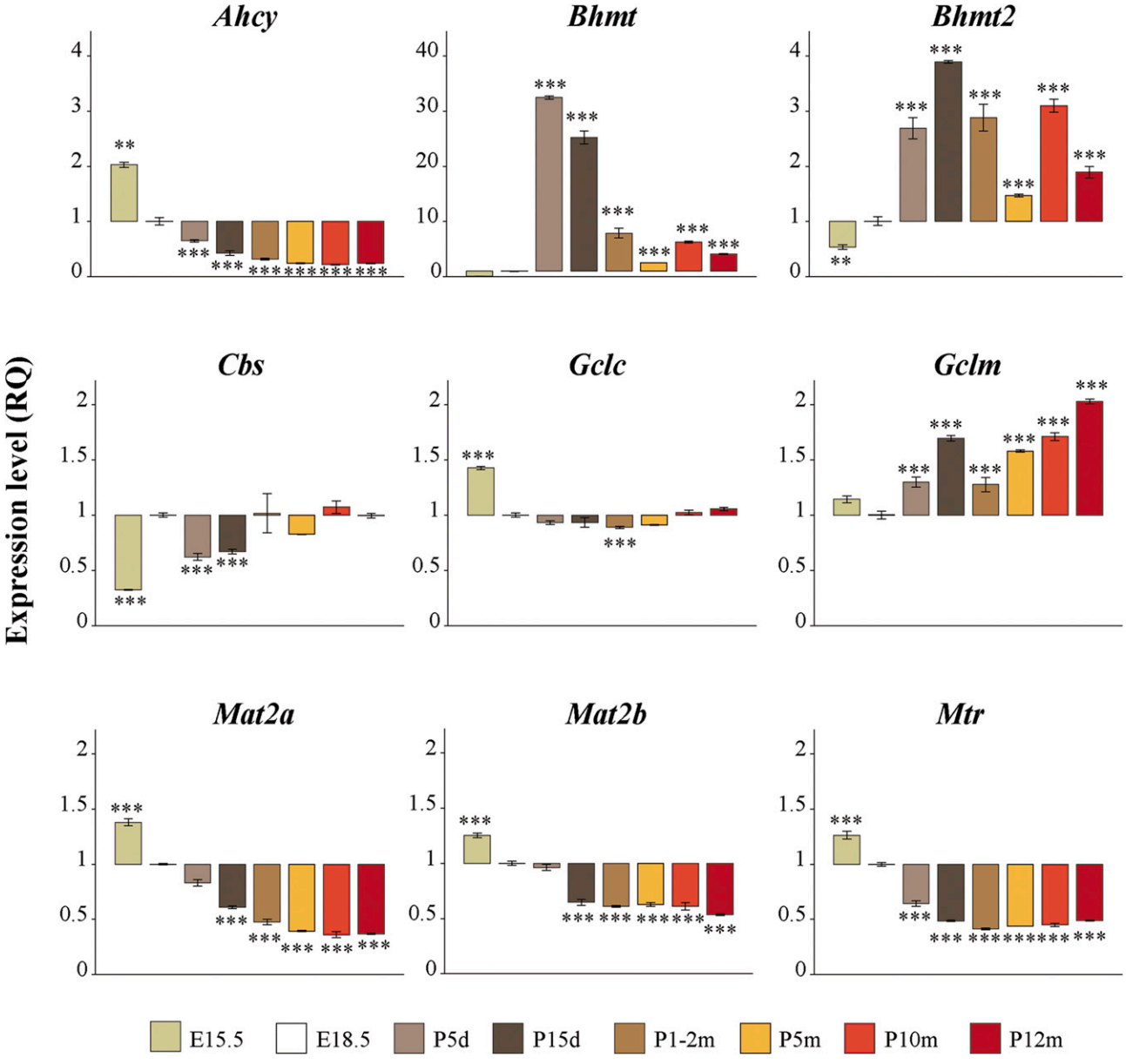

Figure 1. Age-regulated cochlear expression of genes coding for methionine cycle enzymes in the MF1:129Sv mouse strain. Gene expression was measured by qRT-PCR in cochlear samples from MF1:129Sv mice from embryonic (E) to postnatal (P) ages, expressed as days or months. Expression levels were calculated as $2^{-\Delta\Delta Ct}$ [relative quantity (RQ)], using *Hprt* as reference gene and normalizing with data from E18.5 samples. Values are presented as mean RQ ± SEM of triplicates from a pool of cochlear samples from 3 mice of each age. Statistical significance was estimated by Student's *t* test, comparing each age group with the E18.5. $^{**}P < 0.01$, $^{***}P < 0.001$.

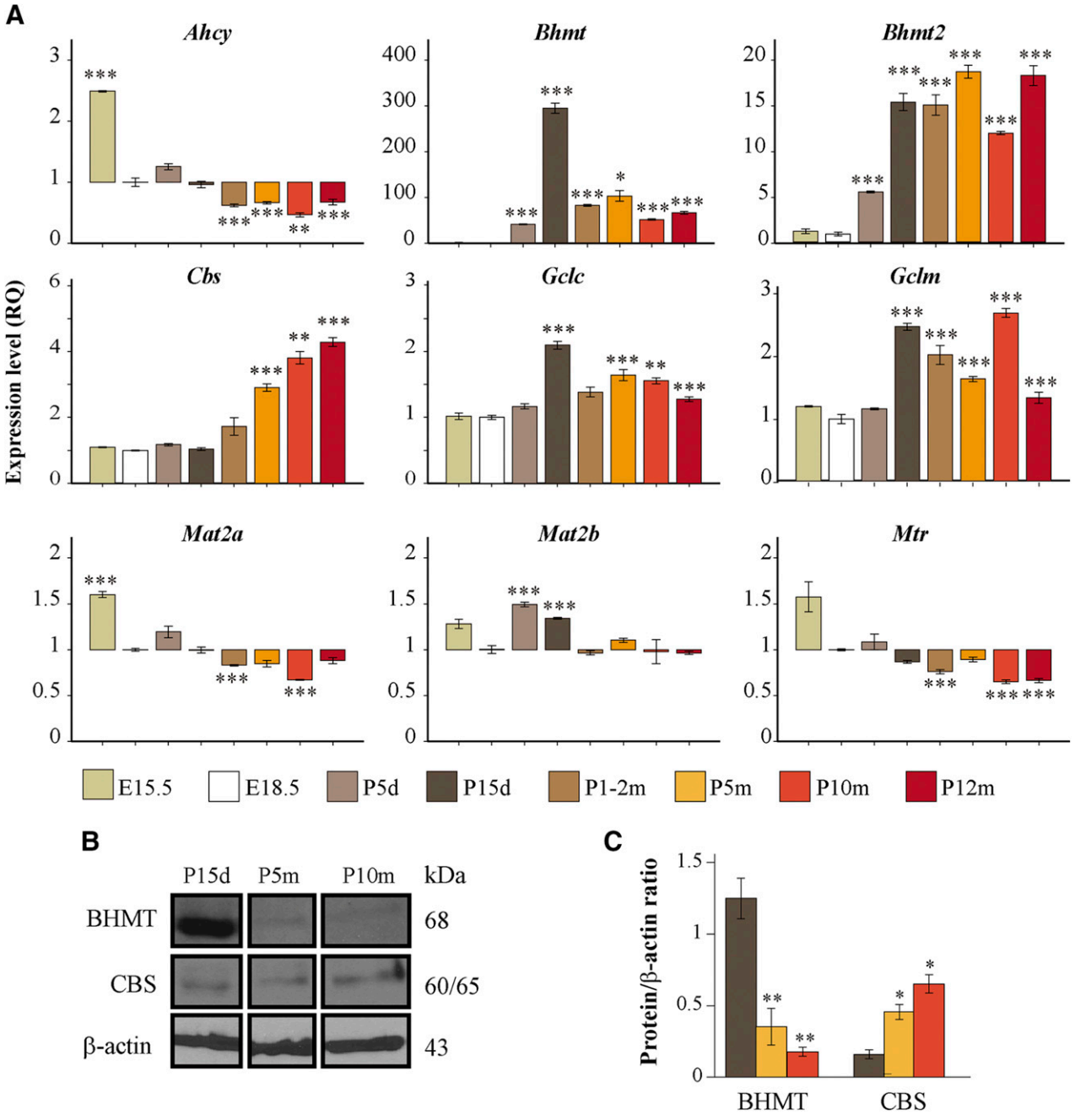

Figure 2. Cochlear gene expression and protein levels of the methionine cycle enzymes in the C57BL/6J mouse strain. *A*) Gene expression was measured by qRT-PCR in cochlear samples from C57BL/6J mice from embryonic (E) to postnatal (P) ages expressed as days or months. RNA was extracted from pools of 3 cochleae from 3 mice of each age. Expression levels were calculated as $2^{-\Delta\Delta Ct}$ [relative quantity (RQ)], using *Hprt* as reference gene and normalizing with data from E18.5 samples. Values are presented as mean RQ ± SEM of triplicates from a pool of cochlear samples from 3 mice per condition. Statistical significance was estimated by Student's *t* test, comparing each age group with the E18.5 *B, C*) Cochlear protein levels in C57BL/6J mice were analyzed by Western blotting using antibodies against BHMT and CBS. Representative immunoblots for each antibody are shown (*B*) together with the quantification [(*C*), $n = 3$ per age]. Data were normalized using β-actin as the loading control. Values are expressed as means ± SEM. Statistical significance was determined by using the Student's *t* test, using P15 data as reference. $^*P < 0.05$, $^{**}P < 0.01$, $^{***}P < 0.001$.

whereas *Gclc*, implicated in glutathione synthesis, presented higher expression levels at embryonic stages. In contrast, *Bhmt* and *Bhmt2*, both also involved in homocysteine remethylation to methionine, showed low expression at fetal stages, an increase in postnatal d 5 and 15, and a gradual decrease thereon. Finally, *Cbs*, first enzyme in the trans-sulfuration pathway, showed a similar profile but with a stable gene expression along the oldest ages studied.

Expression patterns of these genes at the E18.5 stage were also confirmed by RNA arrays using C57BL/6J mouse cochleae, a well-known inbred strain that shows early age-related hearing loss (48). In this case, the most expressed genes were *Ahcy*, *Mat2a*, and *Mat2b* from the

TABLE 1. *Transcription levels of methionine metabolism genes in the cochlea of E18.5 mice*

Symbol	Gene name	Expression level
Ahcy	*S*-adenosylhomocysteine hydrolase	8.64 ± 0.02
Ahcy1	*S*-adenosylhomocysteine hydrolase-like 1	7.98 ± 0.05
Amd1	*S*-adenosylmethionine decarboxylase 1	8.77 ± 0.01
Apip	Apoptotic peptidase activating factor 1 (APAF1) interacting protein	7.22 ± 0.12
Bhmt	Betaine-homocysteine methyltransferase	2.74 ± 0.10
Bhmt2	Betaine-homocysteine methyltransferase 2	1.92 ± 0.10
Carm1	Coactivator-associated arginine methyltransferase 1	8.44 ± 0.07
Cbs	Cystathionine β-synthase	2.10 ± 0.29
Cdo1	Cysteine dioxygenase 1, cytosolic	8.26 ± 0.05
Cth	Cystathionase (cystathionine γ-lyase)	4.93 ± 0.04
Dnmt1	DNA methyltransferase (cytosine-5) 1	8.42 ± 0.02
Dnmt3a	DNA methyltransferase 3A	8.21 ± 0.04
Dnmt3b	DNA methyltransferase 3B	4.96 ± 0.10
Gclc	Glutamate-cysteine ligase, catalytic subunit	6.95 ± 0.03
Gclm	Glutamate-cysteine ligase, modifier subunit	7.22 ± 0.03
Got1	Glutamate oxaloacetate transaminase 1, soluble	7.15 ± 0.04
Got2	Glutamate oxaloacetate transaminase 2, mitochondrial	9.92 ± 0.03
Gnmt	Glycine N-methyltransferase	0.69 ± 0.29
Mat1a	Methionine adenosyltransferase I, α subunit	0.00 ± 0.33
Mat2a	Methionine adenosyltransferase II, α subunit	8.83 ± 0.08
Mat2b	Methionine adenosyltransferase II, β subunit	7.64 ± 0.03
Mcee	Methylmalonyl coenzyme A epimerase	7.52 ± 0.02
Msrb2	Methionine sulfoxide reductase B2	6.26 ± 0.11
Mtap	Methylthioadenosine phosphorylase	6.80 ± 0.07
Mtfmt	Mitochondrial methionyl-tRNA formyltransferase	6.73 ± 0.08
Mthfr	5,10-Methylenetetrahydrofolate reductase	7.99 ± 0.03
Mtrr	5-Methyltetrahydrofolate-homocysteine methyltransferase reductase	6.05 ± 0.10
Mut	Methylmalonyl-Coenzyme A mutase	7.54 ± 0.03
Pcca	Propionyl Coenzyme A carboxylase, α polypeptide	8.00 ± 0.02
Pccb	Propionyl Coenzyme A carboxylase, β polypeptide	7.91 ± 0.12
Pemt	Phosphatidyl ethanolamine methyl transferase	4.08 ± 0.08
Rnmt	RNA (guanine-7-) methyltransferase	7.24 ± 0.04
Shmt1	Serine hydroxymethyl transferase 1 (soluble)	6.37 ± 0.04
Sms	Spermine synthase	5.12 ± 0.06
Srm	Spermidine synthase	9.12 ± 0.02
Suox	Sulfite oxidase	6.33 ± 0.07
Tat	Tyrosine aminotransferase	2.58 ± 0.11

Gene expression was determined using the whole-transcriptome GeneChip Mouse Genome 430A 2.0 Array. RNA was isolated from 3 independent cochleae pools from C57BL/6J E18.5 mouse embryos (n = 6). Gene expression data of methionine cycle and related metabolic pathways were analyzed by puma Bioconductor package to obtain an expression level for the different probe sets on each array. Previously collected expression data from the different replicates were combined with the Probability of Positive Log Ratio (PPLR) method to give a single expression level (mean ± SD), as it is included in the table.

methionine cycle, followed by *Gclc*, *Gclm*, and 5-methyltetrahydrofolate-homocysteine methyltransferase reductase from the folate cycle and glutathione synthesis. In contrast, *Bhmt* and *Bhmt2* (from the methionine cycle) and *Cbs* (trans-sulfuration pathway) showed a low expression in the prenatal cochlea (Table 1). Further analysis in this strain during aging was again carried out using qRT-PCR. Similar age-related transcription profiles were obtained for most of the methionine metabolism genes, except for of *Cbs* and *Gclc*. Thus, *Ahcy*, *Mat2a*, and *Mtr* showed high expression levels in embryonic stages that decrease with age, and *Bhmt* and *Bhmt2* presented high levels in perinatal phases. *Mat2b* expression was sustained postnatally until the age of 1–2 mo, to then decrease. *Cbs* and *Gclc*, which had small expression changes in MF1:129Sv mice, showed strong changes in C57BL/6J mice during aging (Fig. 2*A*). Interestingly, although the expression profiles were similar in both mouse strains, the relative levels of *Bhmt* and *Bhmt2* transcription increased by 10 and 5 times, respectively, in C57BL/6J cochleae. Next, we measured cochlear protein levels of BHMT and CBS by Western blotting. The results confirmed that the levels of theses enzymes were age regulated, with BHMT decreasing and CBS increasing over time (Fig. 2*B, C*).

These data, along with previous reports linking BHMT deficiency with hearing loss (8, 10), prompted us to study the hearing phenotype of the *Bhmt* $^{-/-}$ null mouse.

BHMT deficiency causes hyperhomocysteinemia but not hearing loss

Young (2–3-mo-old) C57BL/6J *Bhmt*$^{-/-}$ mice showed increased concentrations of plasma homocysteine compared with their wild-type littermates, confirming

previous reports (49) (**Fig. 3*A***). To establish whether hyperhomocysteinemia affected auditory function, hearing was assessed by ABR in *Bhmt*$^{-/-}$ and wild-type mice (Fig. 3*B–D*). There was no correlation between plasma homocysteine levels and ABR thresholds (Pearson's correlation coefficient $r = 0.283$; $P = 0.153$). Mice from both genotypes showed similar ABR wave patterns (Fig. 3*B*) and hearing thresholds in response to click and pure tones (Fig. 3*C*). There were no differences in the auditory phenotype of male and female mice, and therefore, both sexes were included in the study (Fig. 3*C*). Similarly, the analysis of wave latencies and amplitudes in response to 70–dB SPL click stimulation (Supplemental Fig. S1 and **Table 2**) did not show significant differences between genotypes at the ages studied.

The C57BL/6J mouse strain presents early age-related hearing loss (48); therefore, the oldest age studied for *Bhmt*$^{-/-}$ and wild-type mice was 5–6 mo old. We observed an increase in high-frequency (20- and 40-kHz) thresholds when compared with 2–3-mo-old mice in both *Bhmt*$^{-/-}$ and wild-type mice. However, no significant differences between genotypes were detected at this age. Therefore, the high levels of plasma homocysteine did not seem to affect cochlear function, at least during the first 6 mo of age.

In accordance with ABR results, no gross alterations in cochlear morphology and cytoarchitecture were observed in the *Bhmt*$^{-/-}$ compared with wild-type mice at the ages studied. However, the expression levels of cochlear cell type–specific markers, including *RbFox3* (*NeuN*) for auditory neurons (38, 39), *Mpz* for Schwann cells (40, 41), *Sox2* for supporting cells (42–44), and *Kcnj10* for stria vascularis intermediate cells (45), but not prestin (solute carrier family 26 member 5) for outer hair cells (46, 47), were lower in 3-mo-old *Bhmt*$^{-/-}$ than wild-type mice (**Fig. 4*A*, *B***). This differential expression suggests the existence of cellular alterations in the *Bhmt*$^{-/-}$ cochlea that could precede functional or morphologic changes. Accordingly, the cochlear expression of methionine metabolism genes in 5–6-mo-old mice showed significantly higher levels of *Mat2a*, *Mat2b*, *Mtr*, *Cbs*, *Gclc*, and *Gclm* in *Bhmt*$^{-/-}$ than in the *Bhmt*$^{+/+}$ mice (Fig. 4*C*).

BHMT deficiency predisposes to increased hearing injury in response to noise exposure

Mice from both genotypes were exposed to noise and, subsequently, plasma homocysteine levels, liver AdoMet, and AdoHcy concentrations and hearing were evaluated at the indicated time points (**Fig. 5*A***). Baseline differences in plasma homocysteine levels in *Bhmt*$^{-/-}$ and wild-type mice were also apparent at 2 and 28 d after noise exposure (Fig. 5*B*). Increased values, but a larger dispersion, were observed after noise exposure in the null mice compared with baseline data. Therefore, there was no correlation between plasma homocysteine levels and ABR thresholds after noise exposure (baseline, $r = 0.194$, $P = 0.568$; 2 d after noise exposure, $r = 0.527$, $P = 0.180$; 28 d after noise exposure, $r = 0.500$, $P = 0.208$). Because the liver is the main contributor to plasma homocysteine levels, the effect of noise exposure on key metabolite levels of the hepatic methionine cycle of *Bhmt*$^{+/+}$ and *Bhmt*$^{-/-}$ mice following this stress were evaluated. Concordantly, the hepatic methylation index (AdoMet/AdoHcy) was greatly reduced in the null mice following noise exposure (Fig. 5*C*).

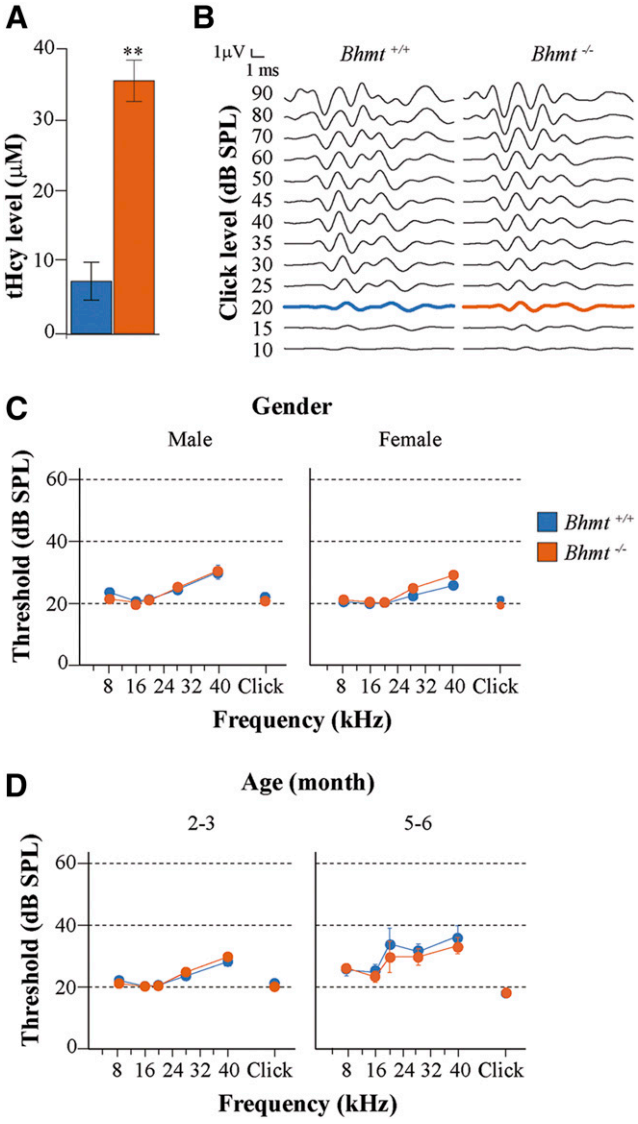

Figure 3. Homocysteine levels and auditory phenotype of the *Bhmt*$^{-/-}$ mouse. *A*) Plasma total homocysteine (tHcy) level was measured by HPLC in 2–3-mo-old *Bhmt*$^{+/+}$ (blue, $n = 5$) and *Bhmt*$^{-/-}$ (orange, $n = 6$) mice. Values are expressed as means ± SEM. Statistical significance was determined using the Mann-Whitney *U* test. $^{**}P < 0.01$. *B*) Hearing evaluation was carried out by ABR recording in both genotypes. Representative waves in response to click at decreasing intensities from 5-mo-old *Bhmt*$^{+/+}$ and *Bhmt*$^{-/-}$ mice, with hearing thresholds highlighted in bold. *C, D*) Hearing thresholds were evaluated in response to click and 8-, 16-, 20-, 28-, and 40-kHz pure tone frequencies in 2–3-mo-old (*Bhmt*$^{+/+}$, $n = 25$ males and 17 females; *Bhmt*$^{-/-}$, $n = 43$ males and 35 females) and 5–6-mo-old ($n = 6$ *Bhmt*$^{+/+}$ and 7 *Bhmt*$^{-/-}$) mice. Data are expressed as means ± SEM. No statistically significant differences were found using the Mann-Whitney *U* test.

No significant differences were observed between genders when genotypes were analyzed independently, nor before or after noise damage (Mann-Whitney *U* test, $P > 0.05$ in all the cases). *Bhmt*$^{-/-}$ mice showed higher hearing thresholds in response to click and tone bursts

TABLE 2. *ABR latencies and amplitudes*

ABR parameter	2–3 mo		5–6 mo	
	$Bhmt^{+/+}$	$Bhmt^{-/-}$	$Bhmt^{+/+}$	$Bhmt^{-/-}$
Interpeak latency (ms)				
I–II	0.958 ± 0.060	0.949 ± 0.039	1.014 ± 0.086	0.983 ± 0.150
II–IV	1.909 ± 0.151	1.727 ± 0.020	1.475 ± 0.108	1.628 ± 0.072
I–IV	2.867 ± 0.162	2.676 ± 0.054	2.488 ± 0.176	2.611 ± 0.151
Amplitude (μV)				
I	2.10 ± 0.55	2.24 ± 0.49	1.56 ± 0.21	1.85 ± 0.56
II	2.06 ± 0.26	1.961 ± 0.18	0.83 ± 0.42	2.04 ± 0.75
IV	1.53 ± 0.37	1.846 ± 0.21	1.36 ± 0.34	1.19 ± 0.28

Interpeak latencies and amplitudes of ABR waves in response to 70 dB SPL click stimulation in $Bhmt^{+/+}$ and $Bhmt^{-/-}$ mice of 2–3 (n = 5–6 per genotype) and 5–6 (n = 4 per genotype) mo of age. Data are expressed as means ± SEM.

stimuli at all times after noise exposure, and a poorer recovery of auditory function, than wild-type mice (Fig. 5*D*). At 2 d after noise, mice from both genotypes showed an increase in ABR thresholds, although thresholds in response to click, 8, and 40 kHz were significantly higher in $Bhmt^{-/-}$ than in wild-type mice. At 2 wk following noise damage, ABR thresholds in response to 16, 20, and 28 kHz were over 60 dB SPL in $Bhmt^{-/-}$ but not in wild-type mice, and significant differences were found in most of the ABR thresholds between genotypes. At 4 wk after noise exposure, permanent threshold shifts in the response to 16 kHz were 42 ± 3 and 21 ± 7 for null and wild-type mice, respectively. In addition, $Bhmt^{-/-}$ mice showed altered ABR recordings, with general lower wave amplitudes and peaks III and IV not clearly detectable when compared with wild-type mice. Standard analysis of peak latencies and amplitudes at different click sound levels did not show statistically significant differences between genotypes before or after noise exposure (Mann-Whitney U test, $P > 0.05$ for all the conditions). The correlation factor (range 0–1, being 1 the optimal correlation) was used to compare the similarity in the waveform of the ABR before and after noise exposure (50); 28 d after noise exposure, the correlation factor was lower in $Bhmt^{-/-}$ mice (mean = 0.31, SD = 0.1) than in wild-type mice (mean = 0.59, SD = 0.41).

Cochlear morphology was assessed 28 d after noise injury (**Fig. 6**). Both genotypes showed loss of outer hair cells in the organ of Corti, fibrocytes type I in the spiral ligament, and basal cells in the stria vascularis after noise exposure, mainly in the basal cochlear turn. Cellular damage was more severe in $Bhmt^{-/-}$ than in wild-type mice, especially in outer hair cells (Fig. 6*A*). Hair cell count on whole-mount preparations confirmed increased outer hair cell loss at the basal turn of the organ of Corti (Fig. 6*B*) and significantly fewer outer hair cells in the 40-kHz region (~60% distance from the apex) in $Bhmt^{-/-}$ mice compared with wild-type mice (Fig. 6*C*). qRT-PCR studies also showed decreased *Sox2* expression in both genotypes.

Finally, the expression of methionine metabolism, apoptosis, and inflammation genes was studied in the cochlea of $Bhmt^{+/+}$ and $Bhmt^{-/-}$ mice exposed to noise (**Fig. 7**). At 2 d after noise damage, $Bhmt^{-/-}$ showed significantly lower expression of *Cbs* than wild-type mice (Fig. 7*A*) along with a higher expression of genes related to apoptosis Hepatitis A virus cellular receptor 1 (Havcr1) [Kidney injury molecule-1 (Kim-1)] and inflammation (*Il6*) (Fig. 7*B*). Interestingly, 28 d after noise exposure, *Cbs* levels recovered, becoming similar in both mouse genotypes, whereas, at this time, a significant increase in the *Bhmt2* transcript was detected in $Bhmt^{-/-}$ mice (Fig. 7*A*). These data suggest that recovery from noise exposure may require homocysteine remethylation, a role that, in the absence of BHMT, could be assumed by increased *Bhmt2* transcription, given that the change in *Mtr* levels is negligible.

DISCUSSION

Sensorineural hearing loss has a multifactorial etiology involving genetic predisposition, age, and multiple environmental factors, which include noise, ototoxic substances, and the nutritional status (51). The first step to develop prevention and repair strategies for intervention before damage becomes irreversible is to further understand the molecular basis of genetic-environmental inter-relationships. Previous studies in mouse strains have shown that low levels of folic acid caused early onset and accelerate the progression of age-related hearing loss, although strain-specific hearing loss patterns were found (10, 11). Here, we have studied the expression of methionine metabolism enzymes in the cochlea along age in 2 reference mouse strains to gain insight into the molecular bases for these differences. Hearing acuity and homocysteine remethylation seemed to be related according to this early work, with this link being carried out by remethylation enzymes MTR and BHMTs, which rely on folate, betaine, or *S*-methylmethionine for their function, respectively (1). Indeed, there is increasing evidence linking hyperhomocysteinemia and sensorineural hearing loss in studies conducted in both patient cohorts and experimental animals (1). Therefore, we have also studied here the knockout mouse for *Bhmt* that shows hyperhomocysteinemia (49) and how this genetic mutation impacts in hearing and in the response to the stressor noise.

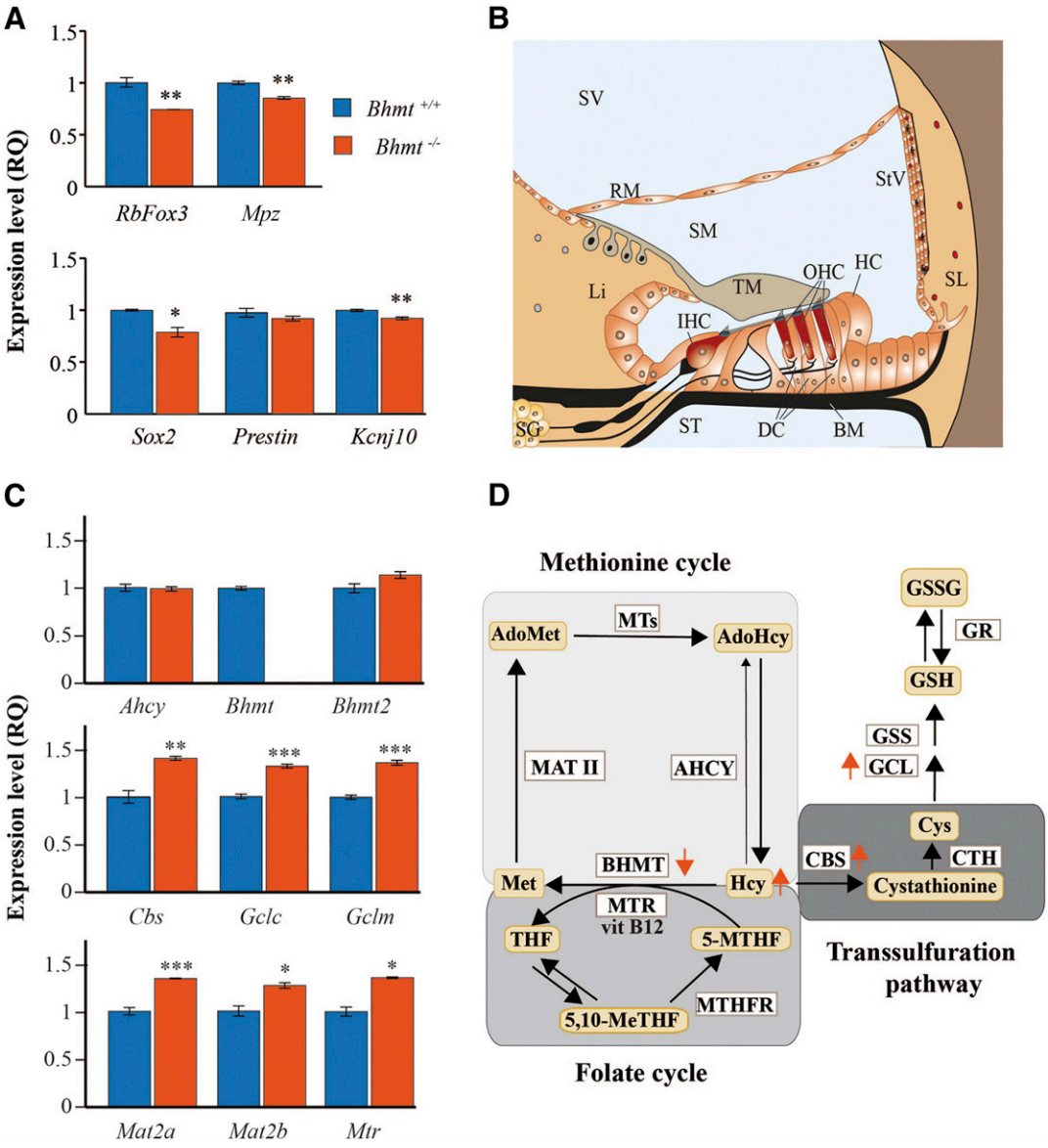

Figure 4. Cell-type biomarkers and methionine metabolism gene expression in the *Bhmt*$^{-/-}$ mouse cochlea. *A*) Cochlear expression of genes encoding for the cell type–specific markers at the spiral ganglia (*RbFox3*, auditory neurons, and *Mpz*; Schwann cells), organ of Corti [*Sox2*, supporting cells, and prestin; outer hair cells (OHCs)], and stria vascularis (*Kcnj10*; intermediate cells) in 3-mo-old mice. Expression levels were calculated as relative quantity (RQ) $2^{-\Delta\Delta Ct}$ in *Bhmt*$^{-/-}$ mice (orange, $n = 3$) relative to the control group, *Bhmt*$^{+/+}$ (blue, $n = 3$), with ribosomal protein large P0 (*Rplp0*) as reference gene. *B*) Schematic drawing of the adult mouse cochlear scala media. BM, basilar membrane; DC, Deiter's cells; HC, Hensen's cells; IHC, inner hair cells; Li, spiral limbus; OHC, outer hair cell; RM, Reisner's membrane; SG, spiral ganglion; SL, spiral ligament; SM, scala media; ST, scala tympani; StV, stria vascularis; SV, scala vestibuli; TM, tectorial membrane. *C*) Expression levels of methionine metabolism genes in 5–6-mo-old mice from both genotypes. *Hprt1* was used as reference gene. *D*) Schematic view of the main metabolic reactions involved in homocysteine (Hcy) metabolism. In the methionine cycle, Hcy is remethylated by the vitamin B_{12}–dependent methionine synthase (MTR) or BHMTs using 5′-methyltetrahydrofolate (5-MTHF) and BHMT or BHMT2 as methyl donors, respectively. Methionine adenosyltransferases (MATs) use methionine (Met) to synthesize AdoMet. Methyltransferases (MTs) transform AdoMet into AdoHcy, which is hydrolyzed by AHCY to produce Hcy in a reversible reaction. Hcy is catabolized by CBS to cystathionine. This metabolite is then utilized by cystathionine γ-lyase (CTH) to produce cysteine (Cys), which can be used for the synthesis of reduced glutathione (GSH) by glutamate-cysteine ligase (GCL) and glutathione synthase (GSS). Oxidized glutathione (GSSG) is reduced by glutathione reductase (GR) using NADPH. The correct function of these pathways depends on a continuous supply of essential nutrients like Met, vitamins B_{12} and B_6, and tetrahydrofolate (THF). In the folate cycle, THF is converted into 5,10-methylenetetrahydrofolate (5,10-MeTHF) and then 5-MTHF in a reaction catalyzed by methylenetetrahydrofolate reductase (MTHFR). Enzymes and metabolites appear in square and rounded boxes, respectively. Orange arrows indicate the main changes in the cochlear expression levels of methionine metabolism genes and in the plasma Hcy levels in the *Bhmt*$^{-/-}$ mice. The lack of BHMT leads to an accumulation of Hcy and favors its secretion to the plasma and conversion to Cys and GSH by an increase in the expression of *Cbs* and *Gcl*, respectively. Values are presented as the means ± SEM of technical triplicates from pooled cochlear samples of 3 mice per genotype. Statistical significance was determined by using the Student's *t* test. $^*P < 0.05$, $^{**}P < 0.01$, $^{***}P < 0.001$

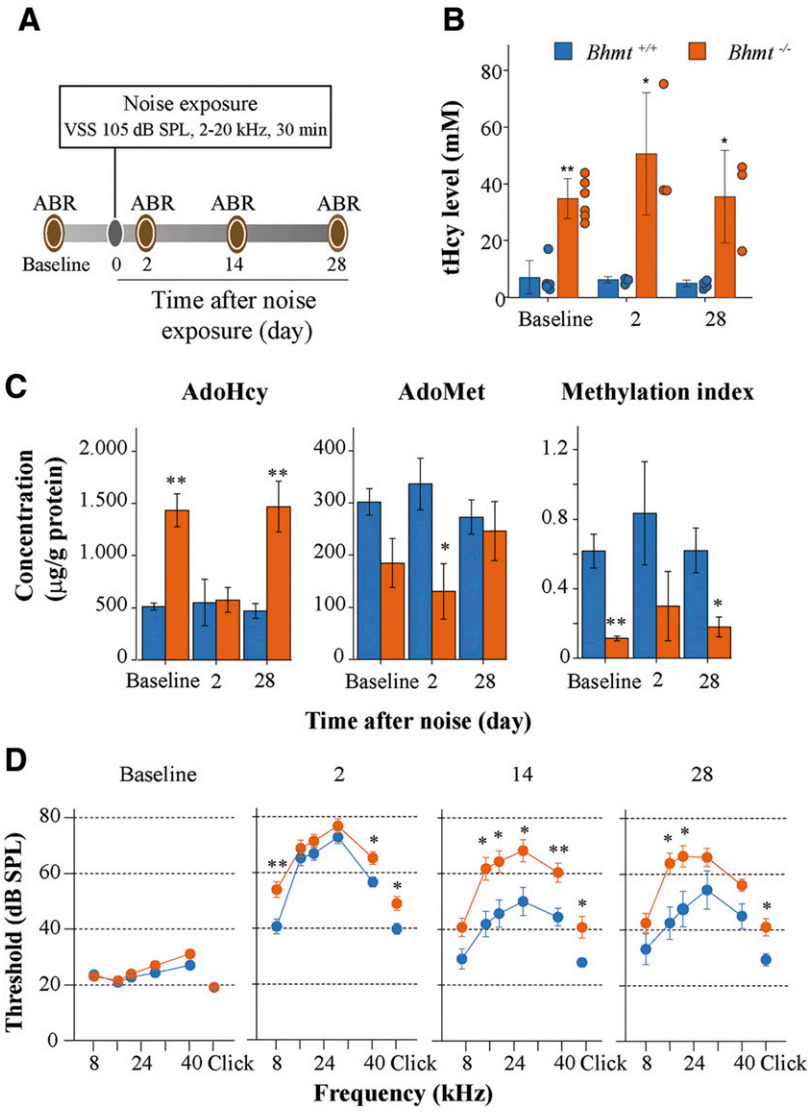

Figure 5. Hearing loss and homocysteine levels in *Bhmt* $^{-/-}$ mice exposed to noise. *A*) Scheme of the experimental workflow. *Bhmt*$^{+/+}$ and *Bhmt*$^{-/-}$ mice (3 mo old) were exposed to violet sweep sine (VSS) noise (105 dB SPL, 2–20 kHz, 30 min). Hearing was assessed by recording ABR before and following exposure to noise. *B*) Plasma total homocysteine (tHcy) level was measured before and 2 and 28 d after exposure to noise in *Bhmt*$^{+/+}$ (blue) and *Bhmt* $^{-/-}$ (orange) mice (n = 3–6 mice of each genotype per moment). *C*) AdoHcy and AdoMet concentration (expressed as micrograms per gram of total protein) was measured in liver samples (n = 5–7 mice of each genotype, per moment) at the same temporal points, and the methylation index (AdoHcy/AdoMet) calculated. *D*) ABR thresholds in response to click and 8-, 16-, 20-, 28- and 40-kHz pure tone frequencies were determined in *Bhmt*$^{+/+}$ (n = 22) and *Bhmt* $^{-/-}$ (n = 23) mice before (baseline) and 2, 14, and 28 d after noise exposure. Data are shown as means ± SEM. Statistical significance was determined by using the Kruskal-Wallis test. $^{*}P < 0.05$, $^{**}P < 0.01$.

Genome expression profiling has been used to identify age-regulated genes in several tissues (52), but the mouse cochlear expression of methionine metabolism genes, to our knowledge, has been not described. Here, we report a comparative study in 2 mouse strains, which differ in the onset and progression of age-related hearing loss, showing that methionine metabolism genes are well represented in the cochlea and are age-regulated. In both strains, *Ahcy*, *Mat2a*, *Mat2b*, and *Mtr* expression levels were high in embryonic stages and decreased with age. In contrast, *Bhmt* and *Bhmt2* transcript levels increased in early postnatal cochlear stages, showing similar profiles but with increased expression in C57BL/6J mice. Liu *et al.* (53) proposed that *Bhmt2* levels and activity are dietary-dependent and adapt to guarantee a lower dependence on folate for homocysteine recycling. Out of the genes studied, the age-modulated profiles of *Cbs* and *Gclc* showed strong differences with the genetic background. Interestingly, the postnatal expression of these 2 genes is increased in the C57BL/6J mouse strain, which is prone to suffer stress damage and early onset of hearing loss (10, 48). CBS is the first enzyme in the trans-sulfuration pathway and directs homocysteine flux toward cysteine and glutathione synthesis. This enzyme contains a heme at the N-terminal domain that regulates the enzyme in response to redox conditions (54). Moreover, *Cbs* heterozygosity is associated with increased cochlear damage and hearing loss (9). On the other hand, *Gclc* is the catalytic subunit of the rate-limiting enzyme in the glutathione synthesis, a tripeptide essential for cell detoxification and antioxidant defense (55). Therefore, the increased expression of these enzymes may be related to their specific functions as compensatory mechanisms that the C57BL/6J mouse cochlea needs to maintain redox balance and thiol status. Furthermore, the increased expression of both *Bhmt* and *Bhmt2* genes along age suggests the additional cochlear need to increase homocysteine recycling to avoid hyperhomocysteinemia. Complementary clinical and basic studies have indicated that hyperhomocysteinemia is a biomarker for human age-associated diseases, particularly cardiovascular disorders and cognitive decline (56, 57). In addition, studies in patients and animal models have shown that the lack of essential micronutrients and cofactors in the methionine metabolism, such as folic acid, leads to

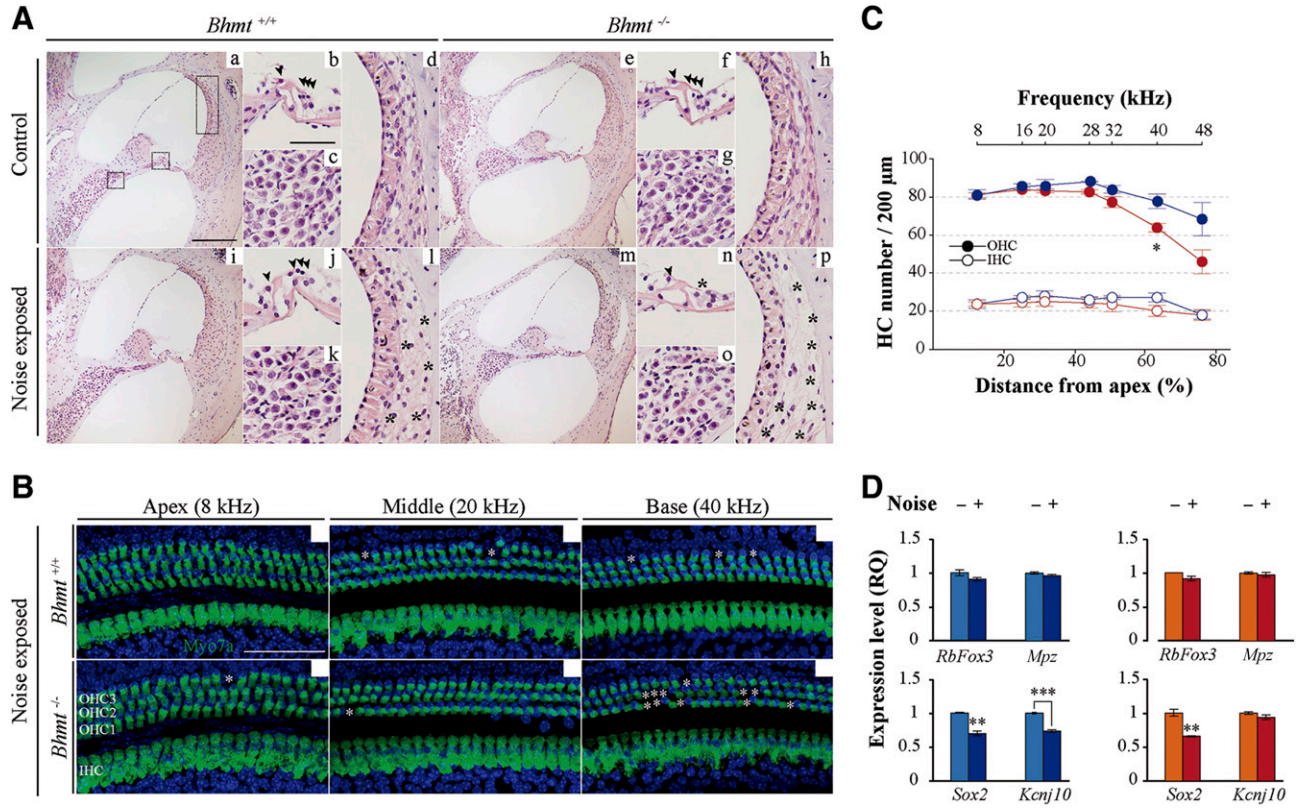

Figure 6. Cochlear morphology of *Bhmt*$^{-/-}$ mice exposed to noise. *A*) Representative microphotographs of hematoxylin and eosin–stained paraffin sections (7 μm) of the basal turn of the cochlea (*a*, *e*, *i*, *m*) and details of the organ of Corti (*b*, *f*, *j*, *n*), spiral ganglion (*c*, *g*, *k*, *o*), and lateral wall (*d*, *h*, *l*, *p*) from mice either nonexposed or exposed to noise from both genotypes 28 d after exposure. Nonexposed control mice showed normal cytoarchitecture in the organ of Corti [arrowheads in *b* point to inner and outer hair cells], spiral ligament, and stria vascularis. After noise exposure, cell loss was observed both genotypes, being the cellular phenotype more evident in *Bhmt*$^{-/-}$ mice (asterisks in *n* and *p*). Scale bar (*a*, *e*, *i*, *m*), 100 μm. Close-up scale bars, 25 μm. *B*) Representative confocal maximal-projection images of the organ of Corti of the apical (8 kHz), middle (20 kHz), and basal (40-kHz) turns of 2–3-mo-old *Bhmt*$^{+/+}$ and *Bhmt*$^{-/-}$ mice 7 d after exposure to noise, immunolabeled for hair cells myosin VIIA (green). Asterisks indicate the absence of outer hair cells. Scale bar, 50 μm. *C*) Number of outer (filled circles) and inner (empty circles) hair cells per 200 μm of basilar membrane quantified in the 8-, 16-, 20-, 28-, 32-, 40- and 48-kHz regions (distance from apex corresponding to the frequencies indicated) in 2–3-mo-old *Bhmt*$^{+/+}$ ($n = 3$) and *Bhmt*$^{-/-}$ ($n = 3$) mice, 7 d after exposure to noise. Values are presented as means ± SEM. *D*) Cochlear gene expression levels were measured by qRT-PCR and expressed as relative quantity (RQ) $2^{-\Delta\Delta Ct}$ in both *Bhmt*$^{-/-}$ (orange, $n = 3$) and *Bhmt*$^{+/+}$ (blue, $n = 3$) mice exposed to noise (dark color) compared with nonexposed controls (light color) 28 d after exposure. Cochlear cell–type biomarkers used were *RbFox3* (*NeuN*) for auditory neurons, *Mpz* for Schwann cells, *Sox2* for supporting cells, and *Kcnj10* for the stria vascularis. ribosomal protein large P0 (*Rplp0*) was used as reference gene. Values are presented as means ± SEM of technical triplicates from pooled cochlear samples of 3 mice per genotype and condition. Statistical significance was determined by using the Student's *t* test. $^{**}P < 0.01$, $^{***}P < 0.001$. Results were considered significant when $P < 0.01$.

hyperhomocysteinemia and an accelerated progression of hearing loss (1, 4–9, 11, 58).

Here, we have studied the impact of the gene deletion and loss of function of BHMT in hearing. *Bhmt* showed the highest cochlear expression of the methionine metabolism genes studied; furthermore, its expression in connexin 30–knockout mice has been related to stria vascularis permeability and hearing loss (8). In our hands and as reported, *Bhmt*$^{-/-}$ mice showed hyperhomocysteinemia and reduced hepatic methylation index (30, 49). However, no evident signs of hearing loss were observed at the ages studied compared with wild-type mice.

Young *Bhmt*$^{-/-}$ mice did not present gross anatomic alterations in the inner ear, but the altered expression of cell type–specific markers suggested the presence of functional loss in the populations of neurons and glial and supporting cells. The stria vascularis was also affected because *Kcnj10* regulates potassium influx and the composition of the endolymph, which is a central factor for cochlear ionic homeostasis (45).

Previous work from our group indicated that folate deficiency induced impaired homocysteine remethylation through BHMT and hyperhomocysteinemia, which in consequence prompted cochlear expression changes directed toward reduction of homocysteine production and elimination through the trans-sulfuration pathway (10). Similar to folate deficiency, *Bhmt*-knockout mice showed decreased homocysteine remethylation and hyperhomocysteinemia. In the same line of evidence, cochlear methionine metabolism in *Bhmt*$^{-/-}$ mice presents a different gene expression profile compared with wild-type mice. *Bhmt* deficiency in the cochlea caused a generalized

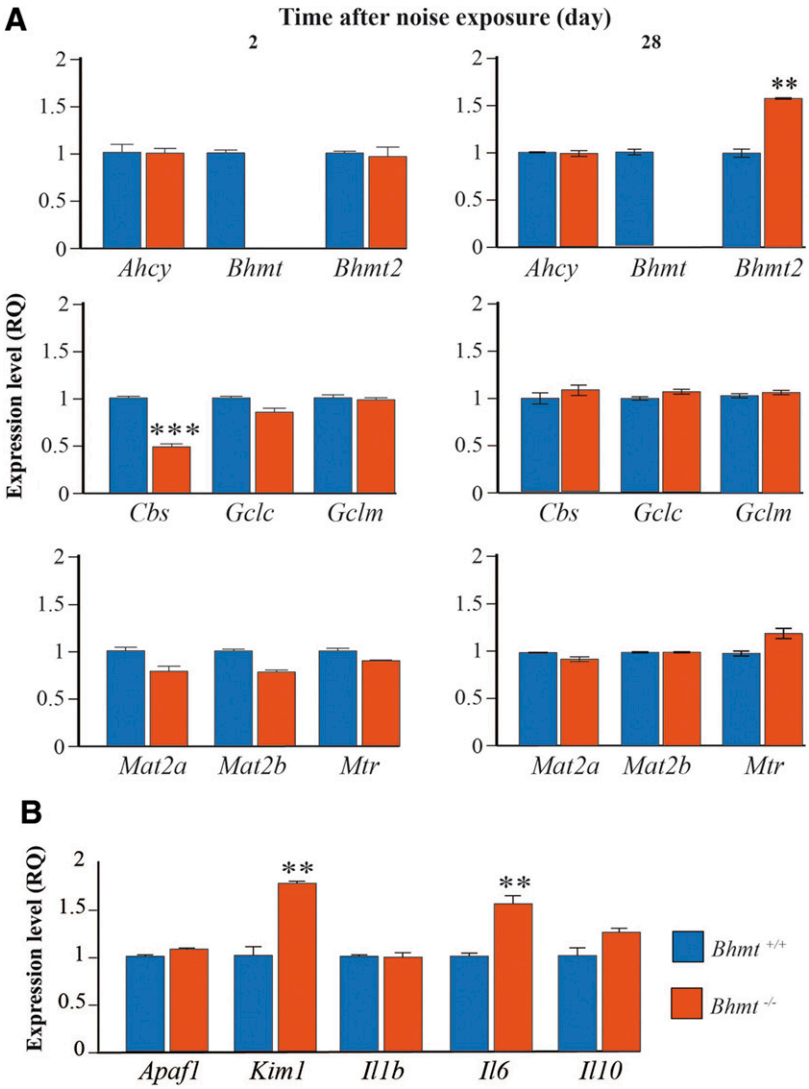

Figure 7. Gene expression response to noise in $Bhmt^{-/-}$ mice. *A*) Cochlear expression of genes coding for methionine metabolism enzymes in $Bhmt^{+/+}$ (blue, $n = 3$) and $Bhmt^{-/-}$ mice (orange, $n = 3$) 2 and 28 d after noise exposure (105 dB SPL, 2–20 kHz, 30 min). Expression levels are represented as $2^{-\Delta\Delta Ct}$ or the *n*-fold difference relative to the $Bhmt^{+/+}$ mice. *B*) Expression of apoptosis and inflammatory genes in the cochlea of $Bhmt^{+/+}$ and $Bhmt^{-/-}$ mice 2 d after noise damage. *Hprt1* was used as reference gene. Values are presented as means ± SEM of triplicates from pooled samples of 3 mice per condition. Statistical significance was determined by using the Student's *t* test. $^{**}P < 0.01$, $^{***}P < 0.001$.

expression increase of the trans-sulfuration pathway genes involved in the synthesis of cysteine and hydrogen sulfide, and therefore glutathione; of *Mtr*, which fulfills an analogous function to that of *Bhmt* in homocysteine remethylation; and of *Mat2* subunits, responsible for the extrahepatic synthesis of AdoMet, the major cellular methyl donor (1). Therefore, although a hearing loss phenotype was not evident, the cochlea of the $Bhmt^{-/-}$ mouse showed notable alterations in methionine metabolism as compared with the C57BL/6J wild type. Interestingly, the tendencies observed in C57BL/6J compared with MF1:129Sv mouse strain appear reinforced in the $Bhmt^{-/-}$ mouse, suggesting chronic subclinical damage.

BHMT human variants have been identified, and some of them have been shown to play a role in the etiology of diseases like certain cancers (59, 60). However, so far there are no published studies showing association of the *BHMT* human variants with progressive hearing loss or susceptibility to noise damage.

Next, we investigated the response of the $Bhmt^{-/-}$ mouse to an otic stressor, noise. There are several lines of work pointing to the existence of relationships between noise exposure and cardiovascular pathology, atherosclerosis, and poor hearing, or vascular disease and age-related hearing loss (12–14, 61). Homocysteine is considered an independent risk factor for cardiovascular disease, but also an agonist of NMDA receptors, which are overexcited in poor hearing (62, 63). Furthermore, hyperhomocysteinemia compromises the integrity of the blood-brain barrier (64), which could explain a reported association between decreased *Bhmt* expression and stria vascularis malfunction (8). Therefore, the defense response of the cochlea could be affected by hyperhomocysteinemia at different levels. In this line of evidence, our data show indeed that BHMT deficiency predisposes to increased hearing injury in response to noise. $Bhmt^{-/-}$ mice presented higher threshold shifts after noise exposure than their wild-type littermates. ABR thresholds after noise exposure showed increased values and a smaller dispersion in the null mice compared with wild-type mice and baseline data. Permanent threshold shifts recorded 28 d after noise exposure also indicated poorer recovery from damage. Quantification in whole

mounts confirmed higher outer hair cell loss in the *Bhmt*$^{-/-}$ than wild-type mice.

Accordingly, *Bhmt*$^{-/-}$ mice showed increased expression of inflammation (*Il6*) and apoptotic markers (*Kim1*) 2 d after noise exposure. Still, cellular alterations did not match an extreme hearing loss phenotype, suggesting that the aforementioned mechanisms, altered barrier integrity, and neuropathy may be contributing. *Bhmt*$^{-/-}$ mice showed higher plasma homocysteine and lower hepatic methylation index than did the wild-type mice at all the times studied. These parameters are not modified following noise exposure in either genotype, although data from knockout mice showed higher dispersion. Interestingly, noise-exposed *Bhmt*$^{-/-}$ mouse cochlea showed a short-term decrease in *Cbs* and long-term increase in *Bhmt2* transcripts. *Cbs* down-regulation impairs trans-sulfuration pathway flux and therefore glutathione synthesis and hydrogen sulfide production. Decrease in glutathione impairs the antioxidant defenses, whereas diminution of hydrogen sulfide alters the cochlear microvasculature. Both changes could contribute to a diminished recovery following damage, due to impaired response to oxidative stress and deficient cell signaling. A recovery of *Cbs* expression levels is observed 28 d after noise exposure, contributing to increased glutathione synthesis and antioxidant defense. On the other hand, the late *Bhmt2* up-regulation could be the result of a higher need for methionine for cochlear recovery (increased methylation needs) and may occur as an attempt to compensate the loss of contribution of BHMT to homocysteine remethylation.

In summary, our data show a direct association between hyperhomocysteinemia and the degree of damage that noise exposure can cause in the mouse cochlea. Therefore, plasma homocysteine levels could be proposed as a prognostic value before potential exposure to noise in the workplace or leisure context. Likewise, our data suggest that nutritional interventions to control homocysteine levels could have a protective value for human hearing. FJ

ACKNOWLEDGMENTS

The authors thank Tania Jareño (Centro de Investigación Biomédica en Red de Enfermedades Raras, CIBERER) for technical support and colleagues at the Neurobiology of Hearing group for sharing data and helpful discussions. The authors thank the Non-invasive Neurofunctional Evaluation and the Genomics facilities [Instituto de Investigaciones Biomédicas Alberto Sols (IIBM), CSIC-UAM] and Histology [Centro Nacional de Biotecnología (CNB), CSIC] for the technical support provided. This work was supported by the Spanish Ministerio de Economía y Competitividad (MINECO)/FEDER SAF2017-86107-R to I.V.-N., U.S. National Institutes of Health (NIH), National Institute of Diabetes and Digestive and Kidney Diseases (Grant DK056350 to S.H.Z.), CEU-Banco Santander precompetitive project (MUSPB047) and CEU-Banco Santander consolidation project (MBS18C12) to T.P., and Puleva BioFoods (to I.V.-N., G.V.-M., and M.A.P.). G.M. was supported by TARGEAR (FP7 PEOPLE 2013 IAPP-612261). The funders had no role in study design, data collection, and analysis, decision to publish, or preparation of the manuscript. The authors declare no conflicts of interest.

AUTHOR CONTRIBUTIONS

T. Partearroyo, S. Murillo-Cuesta, S. H. Zeisel, M. A. Pajares, G. Varela-Moreiras, and I. Varela-Nieto designed the research; T. Partearroyo, S. Murillo-Cuesta, N. Vallecillo, J. M. Bermúdez-Muñoz, L. Rodríguez-de la Rosa, G. Mandruzzato, and A. M. Celaya performed the research; S. H. Zeisel, M. A. Pajares, and I. Varela-Nieto contributed new reagents or analytic tools; T. Partearroyo, S. Murillo-Cuesta, N. Vallecillo, J. M. Bermúdez-Muñoz, L. Rodríguez-de la Rosa, G. Mandruzzato, and I. Varela-Nieto analyzed data; T. Partearroyo, S. Murillo-Cuesta, and I. Varela-Nieto wrote the manuscript; and all authors revised and approved the manuscript.

REFERENCES

1. Partearroyo, T., Vallecillo, N., Pajares, M. A., Varela-Moreiras, G., and Varela-Nieto, I. (2017) Cochlear homocysteine metabolism at the crossroad of nutrition and sensorineural hearing loss. *Front. Mol. Neurosci.* **10**, 107
2. Attias, J., Raveh, E., Aizer-Dannon, A., Bloch-Mimouni, A., and Fattal-Valevski, A. (2012) Auditory system dysfunction due to infantile thiamine deficiency: long-term auditory sequelae. *Audiol. Neurotol.* **17**, 309–320
3. Emmett, S. D., and West, K. P., Jr. (2014) Gestational vitamin A deficiency: a novel cause of sensorineural hearing loss in the developing world? *Med. Hypotheses* **82**, 6–10
4. Houston, D. K., Johnson, M. A., Nozza, R. J., Gunter, E. W., Shea, K. J., Cutler, G. M., and Edmonds, J. T. (1999) Age-related hearing loss, vitamin B-12, and folate in elderly women. *Am. J. Clin. Nutr.* **69**, 564–571
5. Lasisi, A. O., Fehintola, F. A., and Yusuf, O. B. (2010) Age-related hearing loss, vitamin B12, and folate in the elderly. *Otolaryngol. Head Neck Surg.* **143**, 826–830
6. Gok, U., Halifeoglu, I., Canatan, H., Yildiz, M., Gursu, M. F., and Gur, B. (2004) Comparative analysis of serum homocysteine, folic acid and vitamin B12 levels in patients with noise-induced hearing loss. *Auris Nasus Larynx* **31**, 19–22
7. Cadoni, G., Agostino, S., Scipione, S., and Galli, J. (2004) Low serum folate levels: a risk factor for sudden sensorineural hearing loss? *Acta Otolaryngol.* **124**, 608–611
8. Cohen-Salmon, M., Regnault, B., Cayet, N., Caille, D., Demuth, K., Hardelin, J. P., Janel, N., Meda, P., and Petit, C. (2007) Connexin30 deficiency causes instrastrial fluid-blood barrier disruption within the cochlear stria vascularis. *Proc. Natl. Acad. Sci. USA* **104**, 6229–6234
9. Kundu, S., Munjal, C., Tyagi, N., Sen, U., Tyagi, A. C., and Tyagi, S. C. (2012) Folic acid improves inner ear vascularization in hyperhomocysteinemic mice. *Hear. Res.* **284**, 42–51
10. Martínez-Vega, R., Garrido, F., Partearroyo, T., Cediel, R., Zeisel, S. H., Martínez-Álvarez, C., Varela-Moreiras, G., Varela-Nieto, I., and Pajares, M. A. (2015) Folic acid deficiency induces premature hearing loss through mechanisms involving cochlear oxidative stress and impairment of homocysteine metabolism. *FASEB J.* **29**, 418–432
11. Martínez-Vega, R., Murillo-Cuesta, S., Partearroyo, T., Varela-Moreiras, G., Varela-Nieto, I., and Pajares, M. A. (2016) Long-term dietary folate deficiency accelerates progressive hearing loss on CBA/Ca mice. *Front. Aging Neurosci.* **8**, 209
12. Johnsson, L. G., and Hawkins, J. E., Jr. (1972) Vascular changes in the human inner ear associated with aging. *Ann. Otol. Rhinol. Laryngol.* **81**, 364–376
13. Makishima, K. (1978) Arteriolar sclerosis as a cause of presbycusis. *Otolaryngology* **86**, ORL322–ORL326
14. Rosen, S., and Olin, P. (1965) Hearing loss and coronary heart disease. *Bull. N. Y. Acad. Med.* **41**, 1052–1068

15. Durga, J., Verhoef, P., Anteunis, L. J., Schouten, E., and Kok, F. J. (2007) Effects of folic acid supplementation on hearing in older adults: a randomized, controlled trial. *Ann. Intern. Med.* **146**, 1–9
16. Jacques, P. F., Selhub, J., Bostom, A. G., Wilson, P. W., and Rosenberg, I. H. (1999) The effect of folic acid fortification on plasma folate and total homocysteine concentrations. *N. Engl. J. Med.* **340**, 1449–1454
17. De Iriarte Rodríguez, R., Magariños, M., Pfeiffer, V., Rapp, U. R., and Varela-Nieto, I. (2015) C-Raf deficiency leads to hearing loss and increased noise susceptibility. *Cell. Mol. Life Sci.* **72**, 3983–3998
18. Murillo-Cuesta, S., Rodríguez-de la Rosa, L., Contreras, J., Celaya, A. M., Camarero, G., Rivera, T., and Varela-Nieto, I. (2015) Transforming growth factor β1 inhibition protects from noise-induced hearing loss. *Front. Aging Neurosci.* **7**, 32
19. Yamasoba, T., Harris, C., Shoji, F., Lee, R. J., Nuttall, A. L., and Miller, J. M. (1998) Influence of intense sound exposure on glutathione synthesis in the cochlea. *Brain Res.* **804**, 72–78
20. Yamasoba, T., Nuttall, A. L., Harris, C., Raphael, Y., and Miller, J. M. (1998) Role of glutathione in protection against noise-induced hearing loss. *Brain Res.* **784**, 82–90
21. Givvimani, S., Munjal, C., Narayanan, N., Aqil, F., Tyagi, G., Metreveli, N., and Tyagi, S. C. (2012) Hyperhomocysteinemia decreases intestinal motility leading to constipation. *Am. J. Physiol. Gastrointest. Liver Physiol.* **303**, G281–G290
22. Iacobazzi, V., Infantino, V., Castegna, A., and Andria, G. (2014) Hyperhomocysteinemia: related genetic diseases and congenital defects, abnormal DNA methylation and newborn screening issues. *Mol. Genet. Metab.* **113**, 27–33
23. Lehotsky, J., Petras, M., Kovalska, M., Tothova, B., Drgova, A., and Kaplan, P. (2015) Mechanisms involved in the ischemic tolerance in brain: effect of the homocysteine. *Cell. Mol. Neurobiol.* **35**, 7–15
24. Perna, A. F., and Ingrosso, D. (2016) Atherosclerosis determinants in renal disease: how much is homocysteine involved? *Nephrol. Dial. Transplant.* **31**, 860–863
25. Schalinske, K. L., and Smazal, A. L. (2012) Homocysteine imbalance: a pathological metabolic marker. *Adv. Nutr.* **3**, 755–762
26. Gopinath, B., Flood, V. M., Rochtchina, E., McMahon, C. M., and Mitchell, P. (2010) Consumption of omega-3 fatty acids and fish and risk of age-related hearing loss. *Am. J. Clin. Nutr.* **92**, 416–421
27. Jencks, D. A., and Mathews, R. G. (1987) Allosteric inhibition of methylenetetrahydrofolate reductase by adenosylmethionine. Effects of adenosylmethionine and NADPH on the equilibrium between active and inactive forms of the enzyme and on the kinetics of approach to equilibrium. *J. Biol. Chem.* **262**, 2485–2493
28. Ou, X., Yang, H., Ramani, K., Ara, A. I., Chen, H., Mato, J. M., and Lu, S. C. (2007) Inhibition of human betaine-homocysteine methyltransferase expression by S-adenosylmethionine and methylthioadenosine. *Biochem. J.* **401**, 87–96
29. Pajares, M. A., and Pérez-Sala, D. (2006) Betaine homocysteine S-methyltransferase: just a regulator of homocysteine metabolism? *Cell. Mol. Life Sci.* **63**, 2792–2803
30. Teng, Y. W., Mehedint, M. G., Garrow, T. A., and Zeisel, S. H. (2011) Deletion of betaine-homocysteine S-methyltransferase in mice perturbs choline and 1-carbon metabolism, resulting in fatty liver and hepatocellular carcinomas. *J. Biol. Chem.* **286**, 36258–36267
31. Cediel, R., Riquelme, R., Contreras, J., Díaz, A., and Varela-Nieto, I. (2006) Sensorineural hearing loss in insulin-like growth factor I-null mice: a new model of human deafness. *Eur. J. Neurosci.* **23**, 587–590
32. García-Alcántara, F., Murillo-Cuesta, S., Pulido, S., Bermúdez-Muñoz, J. M., Martínez-Vega, R., Milo, M., Varela-Nieto, I., and Rivera, T. (2017) The expression of oxidative stress response genes is modulated by a combination of resveratrol and N-acetylcysteine to ameliorate ototoxicity in the rat cochlea. *Hear. Res.* **358**, 10–21
33. Fell, D., Benjamin, L. E., and Steele, R. D. (1985) Determination of adenosine and S-adenosyl derivatives of sulfur amino acids in rat liver by high-performance liquid chromatography. *J. Chromatogr. A* **345**, 150–156
34. Liberman, M. C., Liberman, L. D., and Maison, S. F. (2014) Efferent feedback slows cochlear aging. *J. Neurosci.* **34**, 4599–4607
35. González, B., Campillo, N., Garrido, F., Gasset, M., Sanz-Aparicio, J., and Pajares, M. A. (2003) Active-site-mutagenesis study of rat liver betaine-homocysteine S-methyltransferase. *Biochem. J.* **370**, 945–952
36. Sanchez-Calderon, H., Rodriguez-de la Rosa, L., Milo, M., Pichel, J. G., Holley, M., and Varela-Nieto, I. (2010) RNA microarray analysis in prenatal mouse cochlea reveals novel IGF-I target genes: implication of MEF2 and FOXM1 transcription factors. *PLoS One* **5**, e8699
37. Pearson, R. D., Liu, X., Sanguinetti, G., Milo, M., Lawrence, N. D., and Rattray, M. (2009) puma: a bioconductor package for propagating uncertainty in microarray analysis. *BMC Bioinformatics* **10**, 211
38. Lin, Y. S., Wang, H. Y., Huang, D. F., Hsieh, P. F., Lin, M. Y., Chou, C. H., Wu, I. J., Huang, G. J., Gau, S. S., and Huang, H. S. (2016) Neuronal splicing regulator RBFOX3 (NeuN) regulates adult hippocampal neurogenesis and synaptogenesis. *PLoS One* **11**, e0164164
39. Pan, H., Song, Q., Huang, Y., Wang, J., Chai, R., Yin, S., and Wang, J. (2017) Auditory neuropathy after damage to cochlear spiral ganglion neurons in mice resulting from conditional expression of diphtheria toxin receptors. *Sci. Rep.* **7**, 6409
40. Liu, Z., Jin, Y. Q., Chen, L., Wang, Y., Yang, X., Cheng, J., Wu, W., Qi, Z., and Shen, Z. (2015) Specific marker expression and cell state of Schwann cells during culture in vitro. *PLoS One* **10**, e0123278
41. Wang, J., Zhang, B., Jiang, H., Zhang, L., Liu, D., Xiao, X., Ma, H., Luo, X., Bojrab D. II, and Hu, Z. (2013) Myelination of the postnatal mouse cochlear nerve at the peripheral-central nervous system transitional zone. *Front Pediatr.* **1**, 43
42. Savoy-Burke, G., Gilels, F. A., Pan, W., Pratt, D., Que, J., Gan, L., White, P. M., and Kiernan, A. E. (2014) Activated notch causes deafness by promoting a supporting cell phenotype in developing auditory hair cells. *PLoS One* **9**, e108160
43. Hume, C. R., Bratt, D. L., and Oesterle, E. C. (2007) Expression of LHX3 and SOX2 during mouse inner ear development. *Gene Expr. Patterns* **7**, 798–807
44. Steevens, A. R., Sookiasian, D. L., Glatzer, J. C., and Kiernan, A. E. (2017) SOX2 is required for inner ear neurogenesis. *Sci. Rep.* **7**, 4086
45. Wangemann, P., Itza, E. M., Albrecht, B., Wu, T., Jabba, S. V., Maganti, R. J., Lee, J. H., Everett, L. A., Wall, S. M., Royaux, I. E., Green, E. D., and Marcus, D. C. (2004) Loss of KCNJ10 protein expression abolishes endocochlear potential and causes deafness in Pendred syndrome mouse model. *BMC Med.* **2**, 30
46. Gross, J., Machulik, A., Amarjargal, N., Fuchs, J., and Mazurek, B. (2005) Expression of prestin mRNA in the organotypic culture of rat cochlea. *Hear. Res.* **204**, 183–190
47. Zheng, J., Shen, W., He, D. Z., Long, K. B., Madison, L. D., and Dallos, P. (2000) Prestin is the motor protein of cochlear outer hair cells. *Nature* **405**, 149–155
48. Kane, K. L., Longo-Guess, C. M., Gagnon, L. H., Ding, D., Salvi, R. J., and Johnson, K. R. (2012) Genetic background effects on age-related hearing loss associated with Cdh23 variants in mice. *Hear. Res.* **283**, 80–88
49. Teng, Y. W., Cerdena, I., and Zeisel, S. H. (2012) Homocysteinemia in mice with genetic betaine homocysteine S-methyltransferase deficiency is independent of dietary folate intake. *J. Nutr.* **142**, 1964–1967
50. Rüttiger, L., Singer, W., Panford-Walsh, R., Matsumoto, M., Lee, S. C., Zuccotti, A., Zimmermann, U., Jaumann, M., Rohbock, K., Xiong, H., and Knipper, M. (2013) The reduced cochlear output and the failure to adapt the central auditory response causes tinnitus in noise exposed rats. *PLoS One* **8**, e57247
51. Bowl, M. R., Simon, M. M., Ingham, N. J., Greenaway, S., Santos, L., Cater, H., Taylor, S., Mason, J., Kurbatova, N., Pearson, S., Bower, L. R., Clary, D. A., Meziane, H., Reilly, P., Minowa, O., Kelsey, L., Tocchini-Valentini, G. P., Gao, X., Bradley, A., Skarnes, W. C., Moore, M., Beaudet, A. L., Justice, M. J., Seavitt, J., Dickinson, M. E., Wurst, W., de Angelis, M. H., Herault, Y., Wakana, S., Nutter, L. M. J., Flenniken, A. M., McKerlie, C., Murray, S. A., Svenson, K. L., Braun, R. E., West, D. B., Lloyd, K. C. K., Adams, D. J., White, J., Karp, N., Flicek, P., Smedley, D., Meehan, T. F., Parkinson, H. E., Teboul, L. M., Wells, S., Steel, K. P., Mallon, A. M., and Brown, S. D. M.; International Mouse Phenotyping Consortium. (2017) A large scale hearing loss screen reveals an extensive unexplored genetic landscape for auditory dysfunction. *Nat. Commun.* **8**, 886
52. Jonker, M. J., Melis, J. P., Kuiper, R. V., van der Hoeven, T. V., Wackers, P. F. K., Robinson, J., van der Horst, G. T., Dollé, M. E., Vijg, J., Breit, T. M., Hoeijmakers, J. H., and van Steeg, H. (2013)

Life spanning murine gene expression profiles in relation to chronological and pathological aging in multiple organs. *Aging Cell* **12**, 901–909
53. Liu, H. H., Lu, P., Guo, Y., Farrell, E., Zhang, X., Zheng, M., Bosano, B., Zhang, Z., Allard, J., Liao, G., Fu, S., Chen, J., Dolim, K., Kuroda, A., Usuka, J., Cheng, J., Tao, W., Welch, K., Liu, Y., Pease, J., de Keczer, S. A., Masjedizadeh, M., Hu, J. S., Weller, P., Garrow, T., and Peltz, G. (2010) An integrative genomic analysis identifies Bhmt2 as a diet-dependent genetic factor protecting against acetaminophen-induced liver toxicity. *Genome Res.* **20**, 28–35
54. Jhee, K. H., and Kruger, W. D. (2005) The role of cystathionine beta-synthase in homocysteine metabolism. *Antioxid. Redox Signal.* **7**, 813–822
55. Lu, S. C. (2013) Glutathione synthesis. *Biochim. Biophys. Acta* **1830**, 3143–3153
56. Koller, A., Szenasi, A., Dornyei, G., Kovacs, N., Lelbach, A., and Kovacs, I. (2018) Coronary microvascular and cardiac dysfunction due to homocysteine pathometabolism; a complex therapeutic design. *Curr. Pharm. Des.* **24**, 2911–2920
57. Sudduth, T. L., Weekman, E. M., Price, B. R., Gooch, J. L., Woolums, A., Norris, C. M., and Wilcock, D. M. (2017) Time-course of glial changes in the hyperhomocysteinemia model of vascular cognitive impairment and dementia (VCID). *Neuroscience* **341**, 42–51
58. Karli, R., Gül, A., and Uğur, B. (2013) Effect of vitamin B12 deficiency on otoacoustic emissions. *Acta Otorhinolaryngol. Ital.* **33**, 243–247
59. Feng, Q., Kalari, K., Fridley, B. L., Jenkins, G., Ji, Y., Abo, R., Hebbring, S., Zhang, J., Nye, M. D., Leeder, J. S., and Weinshilboum, R. M. (2011) Betaine-homocysteine methyltransferase: human liver genotype-phenotype correlation. *Mol. Genet. Metab.* **102**, 126–133
60. Li, F., Feng, Q., Lee, C., Wang, S., Pelleymounter, L. L., Moon, I., Eckloff, B. W., Wieben, E. D., Schaid, D. J., Yee, V., and Weinshilboum, R. M. (2008) Human betaine-homocysteine methyltransferase (BHMT) and BHMT2: common gene sequence variation and functional characterization. *Mol. Genet. Metab.* **94**, 326–335
61. Wu, X., Yang, D., Fan, W., Fan, C., and Wu, G. (2017) Cardiovascular risk factors in noise-exposed workers in China: small area study. *Noise Health* **19**, 245–253
62. Lipton, S. A., Kim, W. K., Choi, Y. B., Kumar, S., D'Emilia, D. M., Rayudu, P. V., Arnelle, D. R., and Stamler, J. S. (1997) Neurotoxicity associated with dual actions of homocysteine at the N-methyl-D-aspartate receptor. *Proc. Natl. Acad. Sci. USA* **94**, 5923–5928
63. Sanchez, J. T., Ghelani, S., and Otto-Meyer, S. (2015) From development to disease: diverse functions of NMDA-type glutamate receptors in the lower auditory pathway. *Neuroscience* **285**, 248–259
64. Kamath, A. F., Chauhan, A. K., Kisucka, J., Dole, V. S., Loscalzo, J., Handy, D. E., and Wagner, D. D. (2006) Elevated levels of homocysteine compromise blood-brain barrier integrity in mice. *Blood* **107**, 591–593

Received for publication September 5, 2018.
Accepted for publication January 15, 2019.